The Journal of Chemical Physics ARTICLE scitation.org/journal/jcp

Role of ripples in altering the electronic and chemical properties of graphene

Cite as: J. Chem. Phys. 156, 054708 (2022); doi: 10.1063/5.0073701
Submitted: 2 October 2021 • Accepted: 14 January 2022 •
Published Online: 3 February 2022

View Online Export Citation CrossMark

Chang-Eun Kim,[1,a)] Jiwoo Lee,[2] Aron Walsh,[2,3] Vincenzo Lordi,[1] and David F. Bahr[4]

AFFILIATIONS

[1] Lawrence Livermore National Laboratory, 7000 East Avenue, Livermore, California 94550, USA
[2] Department of Materials Science and Engineering, Yonsei University, Seoul 07322, South Korea
[3] Department of Materials, Imperial College London, London SW7 2AZ, United Kingdom
[4] School of Materials Engineering, Purdue University, West Lafayette, Indiana 47906-2045, USA

[a)] **Author to whom correspondence should be addressed:** kim87@llnl.gov

ABSTRACT

Ripples of graphene are known to manipulate electronic and hydrogenation properties of graphitic materials. More detailed work is needed to elucidate the structure–property relationship of these systems. In this work, the density functional theory is used to compute the energy and electronic structure of the graphene models with respect to variable curvatures and hydrogen adsorption sites. The magnitude of finite bandgap opening depends on the orientation of ripples, and the hydrogen adsorption energy depends on the local curvature of graphene. An adsorbed hydrogen alters the local curvature, resulting in relatively weakened adsorption on the neighboring three sites, which gives a rationale to experimentally observed dynamic equilibrium stoichiometry (H:C = 1:4) of hydrogenated graphene. The surface diffusion transition state energy of adsorbed hydrogen is computed, which suggests that the Eley–Rideal surface recombination mechanism may be important to establish the dynamic equilibrium, instead of the commonly assumed Langmuir–Hinshelwood mechanism.

Published under an exclusive license by AIP Publishing. https://doi.org/10.1063/5.0073701

INTRODUCTION

Graphene is a two-dimensional material that has high electric conductivity and high chemical stability that originate from its stable resonant bonding structure that features sp^2 hybridization. This carbon-based material is considered a building block for the next generation nano-electronics.[1,2]

Like a thin sheet of fabric, graphene can form ripples[3]—as experimentally confirmed by transmission electron microscopy[4]—but their role in manipulating the properties of graphene has not been understood well. Periodic ripples in graphene open a finite bandgap,[5,6] but detailed investigation into the relationship between the curvature of ripples and the magnitude of the bandgap is needed. Ripples are thought to affect hydrogenation of graphene,[7] and hydrogenation is also known to create a bandgap,[8] but the relation between the local curvature and the hydrogen adsorption energy has not yet established. Ripples can occur over multiple length scales, some of which are even considered as an intrinsic feature of graphene.[9,10] Incomplete knowledge of the structure–property relationships due to ripples in graphene could be more problematic for delicate nano-electronics problems. However, experimental controls over curvature, orientation, and hydrogenation of a graphene are a daunting task, which may be too expensive to repeat over sizable parameter space. We need an accurate yet feasible assessment of this unknown structural parameter space of graphene.

In this work, we use the density functional theory (DFT) to fill the knowledge gap.[11,12] The DFT computes the energy and electronic property of the model atomic structure, from which we can determine the bandgap, hydrogen adsorption energy, and surface diffusion transition states, all with respect to local curvature and ripple orientation. We predict a few important properties of rippled graphene with respect to the local curvature and orientation. Based on the result, we further discuss the rationale behind the experimentally observed dynamic equilibrium of partial hydrogenation,[13] the origin of reversibility,[14] and the preference between Langmuir–Hinshelwood (LH) and Eley–Rideal (ER) surface recombination mechanisms of the adsorbed hydrogen.

METHODOLOGY

We consider two orthogonal ripple propagation directions as expressed by unit cell vector $v_1 = (1, 1)$ and $v_2 = (1, 0)$. In the Miller

Published under an exclusive license by AIP Publishing

notation, the former propagates the ripple along ⟨$\bar{2}$110⟩ or commonly known as zigzag direction, and the latter propagates along ⟨$\bar{1}$100⟩ or armchair direction. The schematic illustrations of these are shown in Fig. 1.

To construct rippled graphene structures for simulation, two different unit cells of graphene are used. A hexagonal unit cell of graphene was expanded by 3 × 10 × 1 times in order to build the zigzag ripple model, and a rectangular unit cell was expanded by 2 × 9 × 1 to build the armchair model. A gamma-centered 4 × 2 × 1 **k**-point grid is used for both the rippled models. For electronic structure calculations, a denser **k**-point grid gamma-centered 8 × 4 × 1 is used, and the linear tetrahedron method with Blöchl correction was used.[15] The initial guess was made by a sinusoidal displacement, but following the force-minimization process found a true ripple structure of graphene for the given boundary constraints. The two models used in the current work have the curvature as C_m = −0.1 and C_m = −0.23, where C_m denotes the curvature at the most concave site of the model.

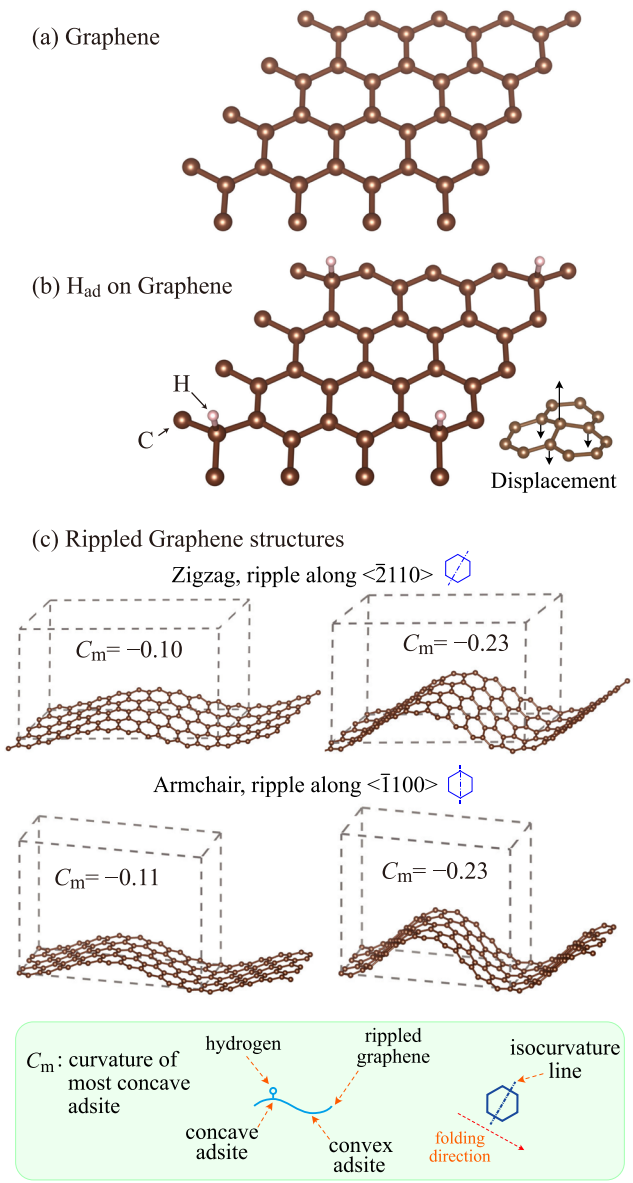

FIG. 1. The curved graphene models: (a) pristine graphene and (b) a hydrogen adatom on graphene. (c) Rippled graphene structures in two folding modes and two different maximum curvatures: zigzag direction and armchair direction. The inset number (C_m) indicates the curvature computed at the most concave sites of the models.

Here, the local curvature C in the unit of (Å^{-1}) is determined in the following way. Ripples propagate along the y axis in the Cartesian coordinate system, and their isocurvature lines are parallel to the x axis. First, we define a cylinder that extends parallel to the x axis and determine the radius of this cylinder when the surface of the cylinder is in contact with three columns of C in rippled graphene models. Then, the distance between the center C column and the center axis of the cylinder is the local radius R, and the local curvature C is $1/R$. The unit of C is omitted throughout the text, in general.

We perform DFT calculations[12] using the generalized-gradient approximation devised by Perdew, Burke, and Ernzerhof (PBE-GGA),[16] as implemented in the Vienna *ab initio* simulation package (VASP).[17,18] Grimme's DFT-D3 scheme was employed to account for the weak van der Waals forces via a London dispersion correction.[19] For most result, we used this PBE-GGA with DFT-D3; however, for the bandgap calculation that will be presented in Fig. 2, concerning that the semi-local approximation could fail to capture the bandgap, we also used the Heyd–Scuseria–Ernzerhof (HSE06) hybrid functional[20–23] to perform self-consistent field calculation using the geometry obtained by the semi-local approximation. Note that for the hybrid functional calculations, a **k**-point grid of gamma-centered 4 × 2 × 1 was used instead of the 8 × 4 × 1 grid.

The kinetic energy cutoff for the plane wave basis set is 500 eV, and the electron–ion interactions are represented using the projector augmented wave (PAW) method. The total energy convergence criterion is 10^{-5} eV for electronic minimization steps and 10^{-4} eV for ionic displacement steps. For **k**-point grids, a gamma-centered 12 × 12 × 1 was used for the graphene unit cell and chair isomer of the graphane unit cell, with the vacuum distance larger than 15 Å. The rippled graphene structures with different orientation and curvature are calculated by minimizing Hellmann–Feynman forces.

The adsorption energy of hydrogen on graphene is calculated as

$$E_{ad}^{H}(C) = E_{tot}^{H-G}(C) - E_{tot}^{G} - E_{tot}^{H_{ref}}, \quad (1)$$

where E_{ad}^{H} denotes the adsorption energy, E_{tot}^{H-G} denotes the total energy of the hydrogenated rippled graphene, C denotes the curvature of the ripple, E_{tot}^{G} denotes the total energy of the rippled graphene, and $E_{tot}^{H_{ref}}$ denotes the total energy of the hydrogen in a reference state. The preferred adsorption site of H on graphene is known to be C top sites,[24] which is implied through the discussions in this paper.

To estimate the energy barrier associated with the diffusion of hydrogen on the rippled structure, we performed a series of climbing image nudged-elastic band (CI-NEB) calculations. We chose ten adsorption sites passing through the most convex to the most concave site using ten images for each segment, yielding 100 images for

Published under an exclusive license by AIP Publishing

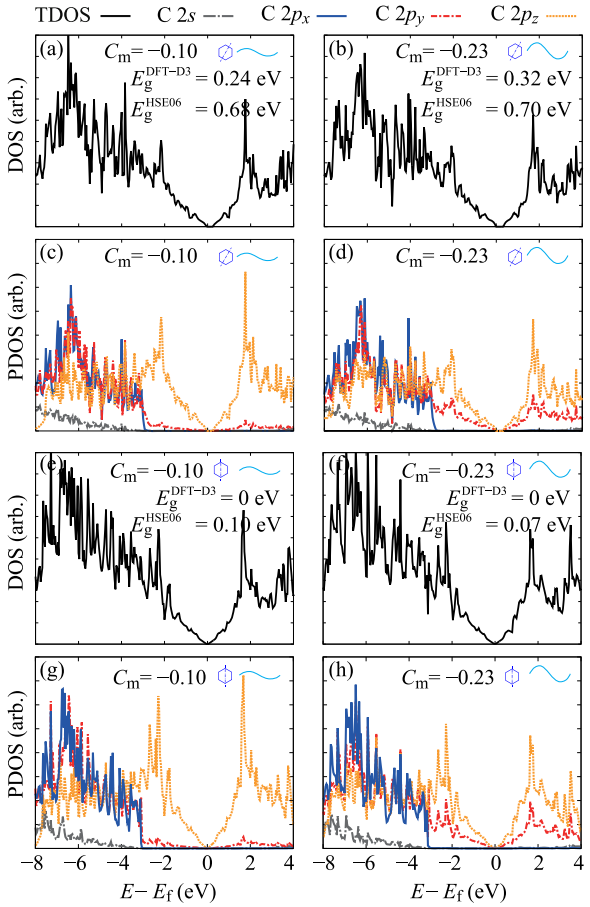

FIG. 2. Calculated electronic density of states (DOS) and projected density of states (PDOS) of curved graphene—rippled along [(a)–(d)] the zigzag direction and [(e)–(h)] the armchair direction. Depending on the folding directions, the magnitude of the finite bandgap varies. Semi-local GGA predicts that the parallel folding modes do not induce a bandgap; however, the hybrid functional (HSE06) predicts that they still obtain a finite bandgap.

each rippled graphene model. The transition image is initially created by linear mixing of the bound images. Up to the second nearest neighbor carbons of the translating hydrogen are fully relaxed to calculate the transition state energy, while higher order neighbors are constrained.

RESULT AND DISCUSSION

In agreement with the experimental observation,[5,6,8,25] rippled graphene has a finite bandgap on the order of 10^{-1} eV, but its magnitude depends on the bending direction—the zigzag direction $\langle\bar{2}110\rangle$ induces a larger gap than the armchair direction (see Fig. 2).

Upon hydrogen adsorption, H 1s overlaps with C 2 p_z to occupy an isolated defect state in the middle of the open bandgap. In comparison, a fully hydrogenated graphene (known as graphane) forms fully overlapping C $2p_z$ and H 1s occupying a low energy valance band, while C $2p_x$ and C $2p_y$ are closer to the Fermi level

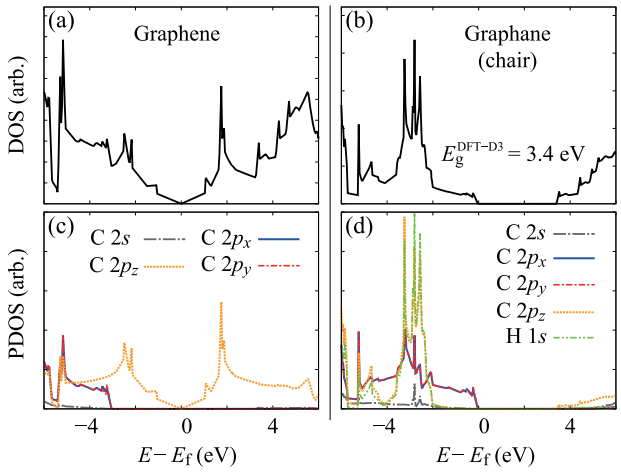

FIG. 3. Calculated electronic density of states (DOS) and projected density of states (PDOS) of [(a) and (c)] flat graphene and [(b) and (d)] graphane. For graphene, the resonant π bondings manifest as prevailing C $2p_z$ states touching at the Fermi level, but for graphane, C $2p_z$ overlaps with H 1s in the localized valence states.

(Figs. 3 and 4). From clean graphene to graphane, H 1s first forms a localized defect state in the middle of the gap for the dilute coverage and then fully overlaps with C $2p_z$ to occupy low energy valance states when fully hydrogenated.

Ripple formation also impacts H adsorption energy (Fig. 5). The adsorption energy is dictated by the local curvature of the C adsite, regardless of the ripple direction. There is this interesting contrast of the two properties: physical bandgap formation is anisotropic, but chemical defect formation is isotropic with respect to the ripple propagation. Note that the adsorption energy takes the reference to the atomic hydrogen state, making it comparable to the experimental condition,[13] but the adsorption energy of molecular hydrogen is endothermic. The initially metastable atomic hydrogen may adsorb on rippled graphene, but as soon as it forms molecular hydrogen, it may leave the surface.

The H adsorption results in notable distortions around the C adsite (Fig. 6). The distorted bonding angles from high concave adsite models allow for a similar bonding angle with those of graphane—compare Figs. 6(a), 6(e), and 6(f)—showing that the concave sites are ideal for forming sp^3 hybridization.

Once adsorbed, the diffusion of H on the surface of rippled graphene is hindered by a barrier as large as 1 eV (Fig. 7). The barrier is still lower than the adsorption energy, which means that the surface hopping of adsorbed hydrogen is not prohibitive.

The anisotropic bandgap formation of rippled graphene may be important to a nanoscale device where 10 meV of the energy gap can make a difference. Intuitively, the bending direction dictates how two neighboring $2p_z$ orbitals interact. The ripple along zigzag $\langle\bar{2}110\rangle$ direction creates the largest gap because it induces direct bending to C–C single bondings, but ripple along armchair $\langle\bar{1}100\rangle$ direction allows the poles of $2p_z$ orbitals to sidestep from each other's bending path. When this is the case, an intermediate rippling direction defined by a linear combination of those two directions may introduce a distinct finite bandgap to the system, introducing an

Published under an exclusive license by AIP Publishing

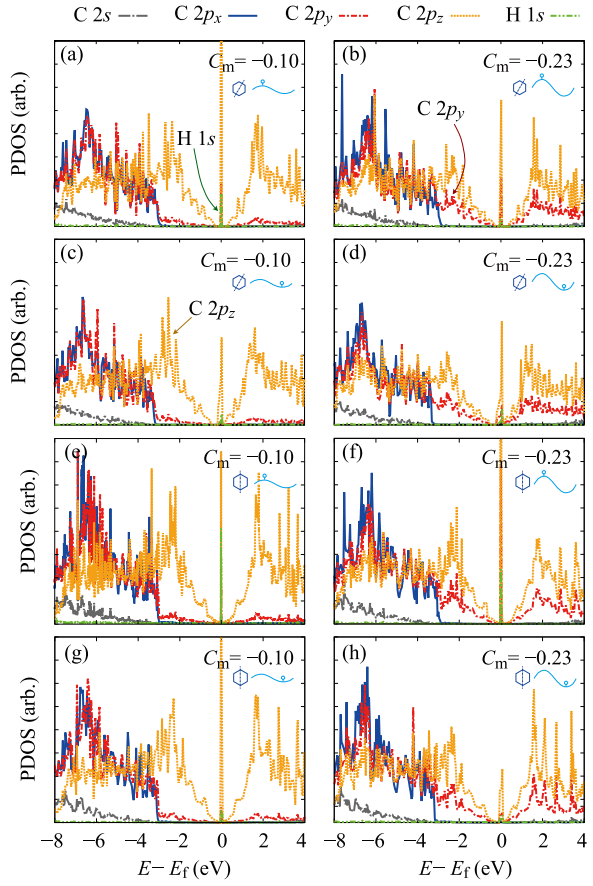

FIG. 4. Calculated electronic density of states (DOS) and projected density of states (PDOS) of the hydrogen-adsorbed rippled graphenes with various curvature and rippling direction—rippled along [(a)–(d)] the zigzag direction and [(e)–(h)] the armchair direction. H adsorption introduces H 1s–C $2p_z$ mixed states at the Fermi level. Higher curvature leads to a more significant overlap of C $2p_y$ with C $2p_z$.

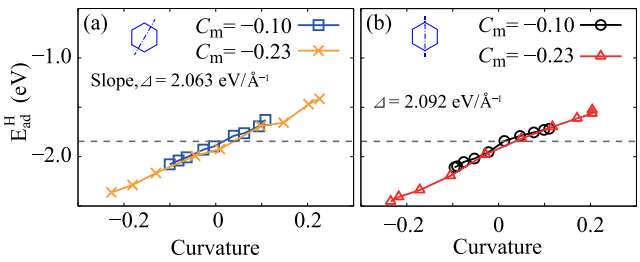

FIG. 5. Calculated adsorption energy of atomic hydrogen on the graphene surface rippled along (a) the zigzag direction and (b) the armchair direction. H adsorb on C top sites, and the adsorption energies are presented with respect to the local curvature of the graphene at each binding site. The gray broken lines indicate the adsorption energy at zero curvature (flat graphene).

additional control parameter to manipulate the electronic property of a rippled graphene device.

Note that within the curvatures used in the present work, the magnitude of the bandgap alone did not scale linearly to the

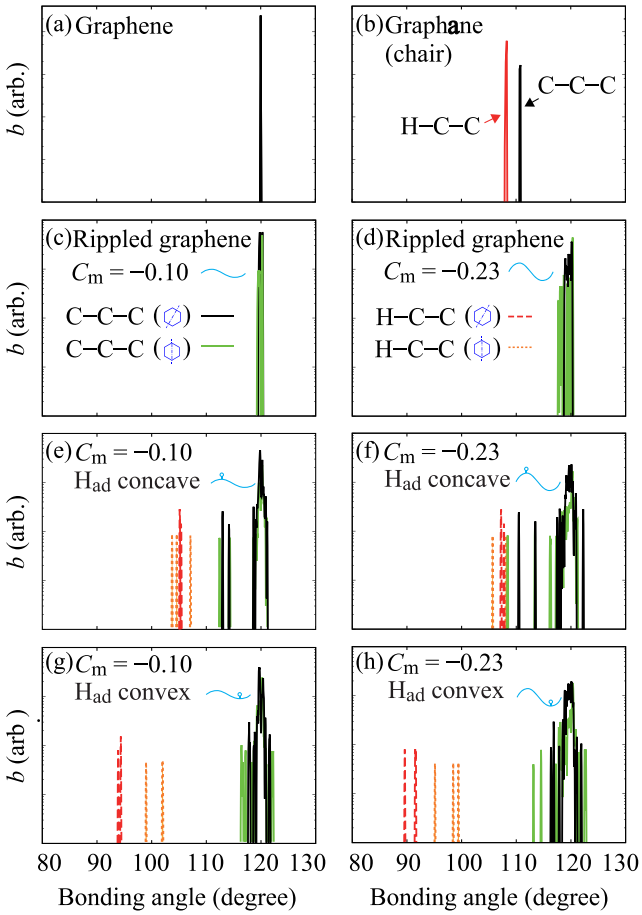

FIG. 6. Bonding angle distributions of (a) graphene, (b) graphane, [(c) and (d)] rippled graphenes with various curvature, and [(e)–(h)] rippled/hydrogen-adsorbed graphene with various curvature and concavity around the adsites. Semi-log scale is used to make relatively small peaks from H–C–C that can be visible. Hydrogen adsorption on the concave sites distorts the local bonding angles toward a resemblance to those of the fully hydrogenated graphane.

curvature and doubling the curvature of the model changes the bandgap only marginally. This makes an interesting comparison to a case of single-walled carbon nanotubes, where the bandgap increases with respect to the decreasing radius of the nanotubes.[26–29] Unlike carbon nanotubes, the curvature of ripple changes its sign alternatively along the propagation axis. The magnitude of the induced bandgap is not a simple function of bending radius (inverse curvature), but it also takes the topology and rippling direction of graphene into account.

Hydrogen adsorption energy on rippled graphene is impacted by ripples, varying as large as 0.8 eV, while the local curvature changes from −0.2 to +0.2. In contrast to the bandgap formation, hydrogen adsorption is not anisotropic, with different rippling directions not creating much difference. Hydrogenation of rippled graphene is a pointwise defect that does not depend on the ripple direction.

Published under an exclusive license by AIP Publishing

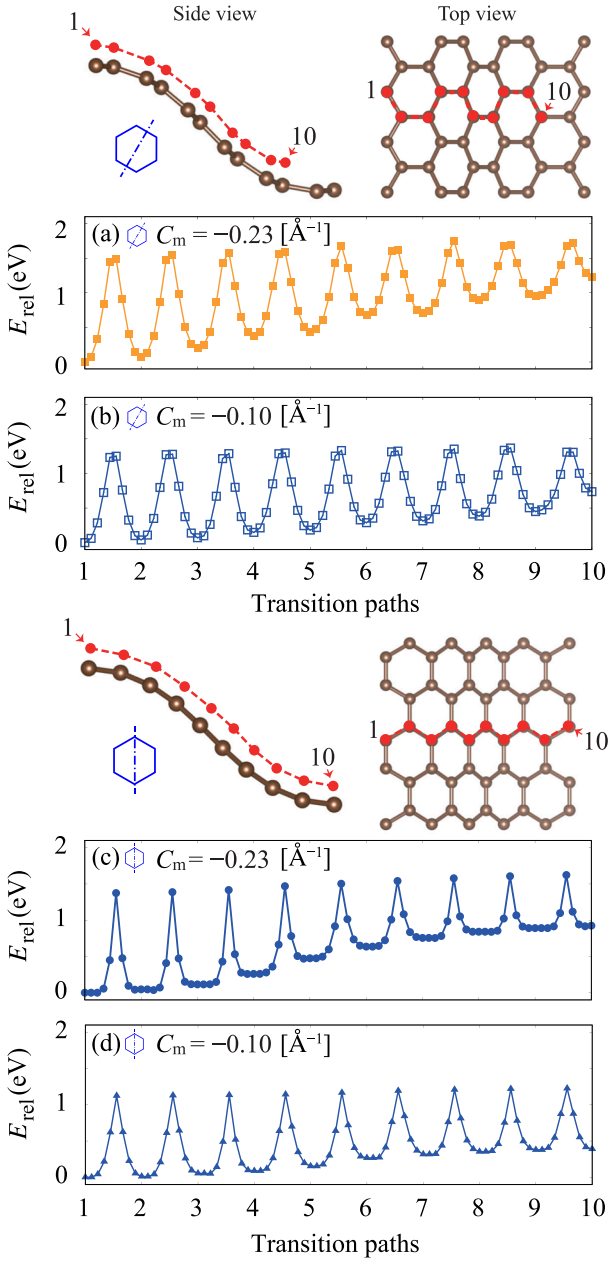

FIG. 7. Transition state energies of hopping adsorbate H on graphene rippled along [(a) and (b)] the zigzag direction and [(c) and (d)] the armchair direction. The folding direction affects the width of the diffusion barriers, while curvature determines relative barrier heights. E_{ref} indicates transition state energy of a hopping H atom on rippled graphene, referenced to the total energy of the adsorption on the adsites with maximum concavity.

These two interesting properties inspire an interesting idea—Is it possible to design a new graphene device that has anisotropic electrical conductivity that is also switchable via chemical modification: anisotropic rippled graphene chemical sensor? In addition, a new mechano-chemical device might be realized by the variable hydrogen adsorption energy with changing local curvature using transverse acoustic vibration to modulate the adsorption energy of chemicals on the surface.

Why does higher curvature allow for stronger H adsorption? From a structural point of view, the higher curvatures should allow for more favorable bonding angles for C sp^3 hybridization (see Fig. 6). From an electronic structure, H 1s states overlap with C $2p_z$ in the middle of the bandgap. We can imagine that more H coverage will result in more overlap of H 1s with C $2p_z$, eventually forming completely overlapping sp^3 hybridization states [see Fig. 3(d)].

All the reported exothermic values shown in Fig. 5 are computed with respect to the atomic hydrogen reference state, in an effort to make it comparable to the atomic beam hydrogenation experiment.[13] However, as soon as we take a reference [$E_{tot}^{H_{ref}}$ term in Eq. (1)] to the molecular state (i.e., $E_{tot}^{H_{ref}} = \frac{1}{2}E_{tot}^{H_2}$, where $E_{tot}^{H_2}$ denotes the total energy of hydrogen molecule), all data shown in Fig. 5 turn to endothermic, suggesting that molecular hydrogen can leave the graphene surface regardless of the local curvature.

The exothermic–endothermic shift by H_2 recombination gives a basis to understand the nature of reversible hydrogenation,[14] where thermal activation can facilitate surface hopping of adsorbed hydrogen, resulting in H_2 recombination followed by desorption. It also provides a possible route to achieve the experimentally observed dynamic equilibrium.[13]

Upon irradiating an atomic beam of hydrogen onto graphene surface, there has been observed a stoichiometric equilibrium of H:C = 1:4. To explain this, we need to relate the adsorption energy, local curvature, and local distortion caused by hydrogen adsorption (Figs. 5 and 6). For each adsorbed H on graphene, it renders three more convex C top sites around each adsite (recall Fig. 6), which means that, for every favorable H adsorption at a given thermodynamic condition, it creates three other more unfavorable H adsites locally. From statistical mechanics point of view, this phenomenon exponentially increases the probability of forming H:C = 1:4. Another contributing factor may be a large surface diffusion barrier. If it were easy for H atoms to jump around and recombine H_2 molecules, they can form molecules and leave the surface, which is not likely to result in a discrete stoichiometry. The surface diffusion barrier of flat graphene is on the same order of magnitude.[30] Relatively, the diffusion barrier from the convex site is much smaller than that from the concave site (recall Fig. 7), which further promote the dynamic equilibrium described above.

With the surface diffusion barrier as high as 1 eV (Fig. 7), the Eley–Rideal (ER) mechanism—where an existing adsorbate combines with an incoming adsorbate—should play a key role in enabling the desorption process to stabilize the dynamic equilibrium, while the Langmuir–Hinshelwood (LH) mechanism—where two existing adsorbates combine to form a molecule—is suppressed by the substantial barrier. Note that for hydrogen, a nuclear quantum effect can modify the diffusion barrier (see a related discussion in Ref. 31) to facilitate quantum tunneling, but this effect is likely to be negligible to the estimated transition state energy.

Rippling is an important feature of 2D materials. The role of ripple is to introduce unique variation of curvature dependent properties to the system. For the case of graphene, a combination of several factors—(1) curvature-dependent adsorption energy, (2) local distortion caused by each adsorption, (3) concavity-dependent

Published under an exclusive license by AIP Publishing

relative diffusion barrier, (4) desorption of molecular hydrogen, and (5) high surface diffusion barrier—contribute to form the experimentally observed dynamic equilibrium of H:C = 1:4. Because adsorption energy is still stronger than the diffusion barrier, thermal activation can still trigger the LH mechanism to form molecular hydrogen to enable "reversible" hydrogenation, but under the condition of continuous flux of the atomic hydrogen beam,[13] the ER mechanism may be more dominant. When all adsorbates leave the surface, the anisotropic electronic property of rippled graphene may recover as well.

The rippling phenomena are not limited to graphene. Other 2D crystalline materials that bend will likely exhibit similar features and deserve further exploration, for which computational materials science tools can be valuable—if not indispensable—leverage to complete our understanding.

CONCLUSION

Periodic ripples of graphene open a finite bandgap, but the magnitude depends on ripple orientation. The zigzag direction, which gives more bending strain to neighboring C–C bonding, creates a larger bandgap. The hydrogen adsorption energy on rippled graphene is strongly affected by the curvature around the adsite carbon. H adsorption leads to bonding angle distortion around the adsite, which resembles that of fully hydrogenated graphene depending on the local curvature of the adsite. The surface diffusion barrier of adsorbed H on rippled graphene is not negligible, as the CI-NEB calculations find higher transition state energy by more than 1 eV. The substantial barrier height signals the need of activation for reversible hydrogenation and suggests that the Eley–Rideal mechanism may be a major desorption mechanism to establish the experimentally observed dynamic equilibrium of the partial hydrogenation.

SUPPLEMENTARY MATERIAL

See the supplementary material for the coordinate data of the four rippled graphene models.

ACKNOWLEDGMENTS

This work was performed under the auspices of the U.S. Department of Energy by Lawrence Livermore National Laboratory under Contract No. DE-AC52-07NA27344.

AUTHOR DECLARATIONS

Conflict of Interest

The authors have no conflicts to disclose.

DATA AVAILABILITY

The data that support the findings of this study are available from the corresponding author upon reasonable request.

REFERENCES

[1] K. S. Novoselov, V. I. Fal'ko, L. Colombo, P. R. Gellert, M. G. Schwab, and K. Kim, Nature **490**, 192 (2012).
[2] A. K. Geim, Science **324**, 1530 (2009).
[3] S. Deng and V. Berry, Mater. Today **19**, 197 (2016).
[4] J. C. Meyer, A. K. Geim, M. I. Katsnelson, K. S. Novoselov, T. J. Booth, and S. Roth, Nature **446**, 60 (2007).
[5] A. Politano and G. Chiarello, Carbon **61**, 412 (2013).
[6] K.-K. Bai, Y. Zhou, H. Zheng, L. Meng, H. Peng, Z. Liu, J.-C. Nie, and L. He, Phys. Rev. Lett. **113**, 086102 (2014).
[7] D. C. Elias, R. R. Nair, T. M. G. Mohiuddin, S. V. Morozov, P. Blake, M. P. Halsall, A. C. Ferrari, D. W. Boukhvalov, M. I. Katsnelson, A. K. Geim, and K. S. Novoselov, Science **323**, 610 (2009).
[8] R. Balog, B. Jørgensen, L. Nilsson, M. Andersen, E. Rienks, M. Bianchi, M. Fanetti, E. Lægsgaard, A. Baraldi, S. Lizzit, Z. Sljivancanin, F. Besenbacher, B. Hammer, T. G. Pedersen, P. Hofmann, and L. Hornekær, Nat. Mater. **9**, 315 (2010).
[9] A. Fasolino, J. H. Los, and M. I. Katsnelson, Nat. Mater. **6**, 858 (2007).
[10] S. Lee, Nanoscale Res. Lett. **10**, 422 (2015).
[11] P. Hohenberg and W. Kohn, Phys. Rev. **136**, B864 (1964).
[12] W. Kohn and L. J. Sham, Phys. Rev. **140**, A1133 (1965).
[13] D. Haberer, C. E. Giusca, Y. Wang, H. Sachdev, A. V. Fedorov, M. Farjam, S. A. Jafari, D. V. Vyalikh, D. Usachov, X. Liu, U. Treske, M. Grobosch, O. Vilkov, V. K. Adamchuk, S. Irle, S. R. P. Silva, M. Knupfer, B. Büchner, and A. Grüneis, Adv. Mater. **23**, 4497 (2011).
[14] S. Ryu, M. Y. Han, J. Maultzsch, T. F. Heinz, P. Kim, M. L. Steigerwald, and L. E. Brus, Nano Lett. **8**, 4597 (2008).
[15] P. E. Blöchl, O. Jepsen, and O. K. Andersen, Phys. Rev. B **49**, 16223 (1994).
[16] J. P. Perdew, K. Burke, and M. Ernzerhof, Phys. Rev. Lett. **77**, 3865 (1996).
[17] G. Kresse and J. Furthmüller, Phys. Rev. B **54**, 11169 (1996).
[18] G. Kresse and J. Furthmüller, Comput. Mater. Sci. **6**, 15 (1996).
[19] S. Grimme, J. Antony, S. Ehrlich, and H. Krieg, J. Chem. Phys. **132**, 154104 (2010).
[20] J. Heyd, G. E. Scuseria, and M. Ernzerhof, J. Chem. Phys. **118**, 8207 (2003).
[21] J. Heyd and G. E. Scuseria, J. Chem. Phys. **121**, 1187 (2004).
[22] J. Heyd, G. E. Scuseria, and M. Ernzerhof, J. Chem. Phys. **124**, 219906 (2006).
[23] J. Paier, M. Marsman, K. Hummer, G. Kresse, I. C. Gerber, and J. G. Ángyán, J. Chem. Phys. **124**, 154709 (2006).
[24] W. Li, L. Huang, M. C. Tringides, J. W. Evans, and Y. Han, J. Phys. Chem. Lett. **11**, 9725 (2020).
[25] U. Monteverde, J. Pal, M. A. Migliorato, M. Missous, U. Bangert, R. Zan, R. Kashtiban, and D. Powell, Carbon **91**, 266 (2015).
[26] C. T. White, D. H. Robertson, and J. W. Mintmire, Phys. Rev. B **47**, 5485 (1993).
[27] R. Saito, G. Dresselhaus, and M. S. Dresselhaus, J. Appl. Phys. **73**, 494 (1993).
[28] H. Ajiki and T. Ando, J. Phys. Soc. Jpn. **62**, 1255 (1993).
[29] C. L. Kane and E. J. Mele, Phys. Rev. Lett. **78**, 1932 (1997).
[30] Y. Han, J. W. Evans, and M. C. Tringides, "Terhmodynamics and kinetics of H adsorption and intercalation for graphene on 6 H-SiC (0001) from first-principles calculations," J. Vac. Sci. Technol. A **40**(1), 012202 (2022).
[31] Y. Han, J. W. Evans, and M. C. Tringides, Appl. Phys. Lett. **119**, 033101 (2021).

Published under an exclusive license by AIP Publishing